Indonesian Journal of Electrical Engineering and Computer Science
Vol. 5, No. 3, March 2017, pp. 556 ~ 563
DOI: 10.11591/ijeecs.v5.i3.pp556-563

An Adaptive Controller for Photovoltaic Emulator using Artificial Neural Network

Razman Ayop*, Chee Wei Tan
Faculty of Electrical Engineering, Universiti Teknologi Malaysia, 81310, Skudai, Johor, Malaysia
Corresponding author, e-mail: razmanayop@gmail.com*, cheewei@utm.my

Abstract

The photovoltaic (PV) emulator is a nonlinear power supply that features the similar characteristic of the PV module. However, the nonlinear characteristic of the PV module causes instability of the PV emulator output. The conventional solution is to operate the PV emulator in the overdamped condition which results in a poor dynamic performance. This drawback is solved by manipulating the proportional and integral gains of the proportional-integral (PI) controller. In this paper, the artificial neural network is used in the adaptive PI controller to maintain a stable and fast dynamic response of the PV emulator. This has been simulated with varied output resistance and irradiance. By comparing the proposed control strategy with the conventional method during start-up response of the photovoltaic emulator, the dynamic performance of the output current has shown an improvement of up to 80 % faster than the conventional method.

Keywords: *PV, PI Controller, Interleaved Buck Converter, Multiple Stage Filter*

1. Introduction

The uses of renewable energy become more popular especially the solar energy due to the increases in the performance of the photovoltaic (PV) module and the power converter. The power produces by the PV module is affected by the weather condition and requires the maximum power point tracking (MPPT) devices and power conditioning system to retrieve the maximum power from the PV module. However, the development of MPPT requires a full control of the factor that affecting the PV module which is the irradiance and module temperature. However, this experimental setup is complex, which requires a large space for the PV module. Moreover, the repetitive testing conditions are difficult to achieve. Due to these drawbacks, the MPPT device tested using the PV emulator would be more cost effective and time-saving.

The common PV emulator consists of a conventional buck converter with the proportional-integral (PI) controller and a reference input from the PV model [1-3]. Although the conventional buck converter is simple and requires a low number of components, the dynamic response is slow due to a large capacitance in order to maintain a small voltage ripple. The multiple-stage interleaved buck converter improves the reliability, efficiency, and transient response of the PV emulator [4]. The interleaved converter produces a lower inductor current ripple. As a result, a smaller capacitance is required to maintain similar ripple factor thus producing a faster transient response. The two-stage LC filter (TSLCF) is also introduced in the PV emulator application to improve the bandwidth of the PV emulator system [5].

The dynamic response of the PV emulator varies depending on output resistance [3], [6-7]. A low load resistance causes the overshoot at the output voltage and output current of the PV emulator. On the other hand, a large load resistance causes the PV emulator to response slower. This problem is overcome by implementing the fuzzy PI controller that adapts to the output resistance [8]. However, the nonlinear characteristic of the PV module also affects the dynamic response of the PV emulator [6]. The overdamped PV emulator output is required to prevent instability of the PV emulator output. Therefore, the dynamic response of the PV emulator becomes slow. To overcome this problem, the control system for the PV emulator not only considers the output resistance, but also the irradiance and temperature. However, by consideration these factors into the controller of the PV emulator, the controller for the PV

Received November 12, 2016; Revised February 2, 2017; Accepted February 20, 2017

emulator becomes very complex. Therefore, the artificial neural network (ANN) is used to overcome the complexity of the PV emulator controller.

In this paper, a fast response PV emulator is proposed by applying an adaptive PI controller optimized using the artificial neural network. The paper only covers the control strategy for the PV emulator at a constant PV module temperature setting of 25 ^{o}C in order to reduce the complexity of the controller design. The proposed control strategy is simulated using MATLAB/Simulink® simulation package. The PV model used to represent PV module is the single diode model [9]. The Sanyo HIP-215NKHE5 PV panel is used for the emulation process [10]. The power converter used for the PV emulator is the two stage interleaved buck converter (TSIBC) with the TSLCF. The operation of the power converter is the discontinuous current mode to allow a fast dynamic response. This paper only focuses on the resistive load. The PV emulator is designed to operate under irradiance and output resistance of 200 W/m^2 to 1000 W/m^2 and 5 Ω to 150 Ω respectively.

2. The Disadvantages of Conventional Control Strategy

The conventional control strategy of the PV emulator system consists of the closed-loop converter system with a PV model as the reference, as shown in Figure 1. Although the control strategy is simple, it suffers from a slow dynamic response and stability problem. There are three disadvantages of the conventional control strategy. The first disadvantage is the output resistance affecting the dynamic response of the system. For the closed-loop controlled system of the TSIBC with the TSLCF, a small output resistance produces a fast dynamic response and a large output resistance produces a slow dynamic response. Therefore, the tuning of PI controller gains is done according to the output resistance to allow the PV emulator to operate at the critically damped operation.

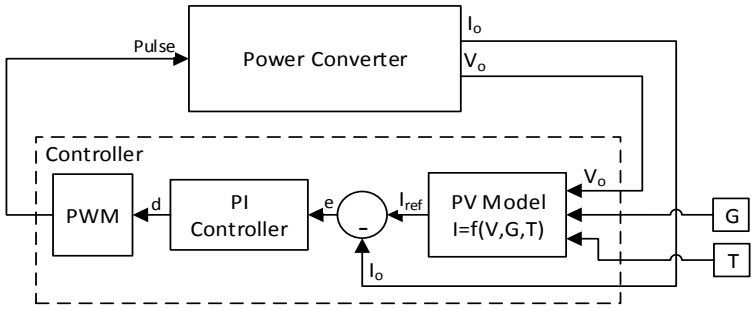

Figure 1. The conventional control strategy of the PV emulator system

The second disadvantage is the different PV emulator output dynamic characteristics is required in the different regions of the current-voltage (I-V) characteristic curve. The PV emulator with the current-controlled system is designed to work at the critically damped operation when the operating point is in the constant current region of the I-V characteristic curve. This is due to a small change in reference current even when there is a large change in the output voltage, as shown in

Figure *2*(a). Therefore, the operation in the constant current region is stable. However, if the PV emulator operates in the constant voltage region, a small change in the output voltage causes a large change in the reference current, as shown in

Figure *2*(a). This causes the reference point to oscillate and the output of the PV emulator become unstable. This problem is overcome by changing the PV emulator controlled system to work at the overdamped operation. However, if the design of the system is overdamped, the dynamic performance of the PV emulator becomes slow. Therefore, the gains of the PI controller need to adapt to the different regions of the PV I-V characteristic curve.

The third disadvantage is the constant current region and constant voltage region depends on the irradiance and temperature. The operating point of the PV emulator with a lower output resistance is near to y-axis of the I-V characteristic curve and a higher output resistance

is near to x-axis of the I-V characteristic curve. The output resistance between the boundary of the constant current region and constant voltage region is called the critical output resistance (R_a and R_b). The PV emulator system is designed to run in critically damped operation when the output resistor is below the critical output resistance. While the PV emulator system is designed to run in overdamped operation when the output resistor is above the critical output resistance to prevent the unstable output of the PV emulator. However, the critical output resistance is changed as the irradiance and PV module temperature setting of the PV emulator changed. The effect of the change in the critical point when the irradiance changed is observed in

Figure *2*(b). Therefore, it is difficult to determine whether the PV emulator system needs to run in critically damped or overdamped operation.

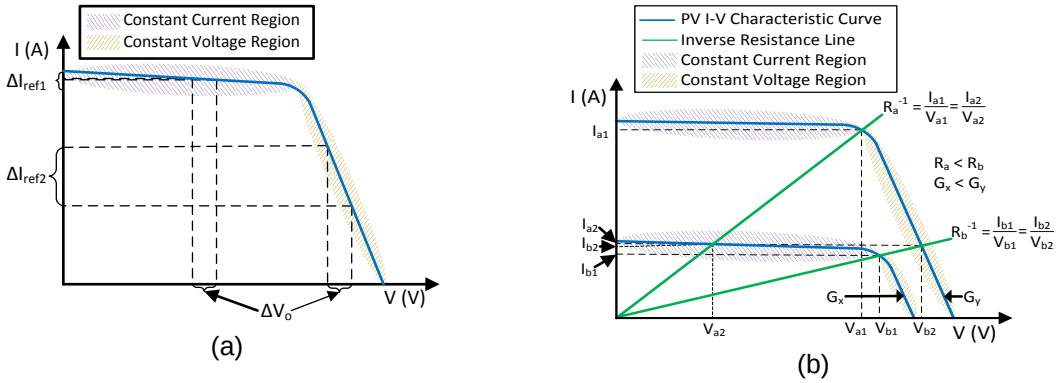

Figure 2. a) The effect of the change in output voltage toward the reference input, I_{ref} in different regions on the PV I-V characteristic curve. b) The change of the boundary location between the constant current region and the constant voltage region on the PV I-V characteristic curved when the irradiance, G is changed

3. The Proposed Control Strategy for the Photovoltaic Emulator

The proposed PV emulator control strategy consists of two parts namely the power converter and the controller. The power converter is the TSIBC with the TSLCF and it is designed to operate with voltage ripple below 2 %. Therefore, the parameters of the power converter are adjusted to achieve this condition, as shown in Table 1.

Table 1. The power converter and the PV model parameters for the PV emulator.

Power Converter

Parameter	Values
Input Voltage, V_i	60 V
Switching Frequency, f	50 kHz
Duty Cycle Limit, D	1 % - 95 %
Inductance (L1, L2, and L3)	50 μH
Inductor Internal Resistance (r_{L1}, r_{L2}, and r_{L3})	0.1 Ω
Capacitance 1 (C1 and C2)	1.4 μF
Equivalent Series Resistor (r_{C1} and r_{C2})	0.1 Ω

PV Model

Parameter	Value
Open Circuit Voltage, V_{oc}	51.6 V
Short Circuit Current, I_{sc}	5.61 A
Maximum Power Point Voltage, V_{mp}	42 V
Maximum Power Point Current, I_{mp}	5.13 A
Temperature Coefficient, K_T	0.129 V/°C

The controller of the PV emulator is consisting of three parts, as shown in Figure 3(a). The first part of the controller is the PV model. The PV model chosen for the study is the single diode model with series and parallel resistance [9]. The PV mathematical equation is shown in Equation 1. The function of the PV model is to produce the reference input according to the PV I-V characteristic curve. The accuracy of the PV emulator is highly affected by the PV model used. The PV panel chosen for the emulation is Sanyo HIP-215NKHE5 PV panel and the parameters for the PV model is shown in Table 1 [10].

$$I_{pv} = I_{ph} - I_s \left[e^{\frac{V_{pv}+I_{pv}R_S}{AV_T}} - 1 \right] - \frac{V_{pv}+I_{pv}R_S}{R_p} \quad (1)$$

Where I_{pv} is the PV current, I_{ph} is the photo-generated current or photocurrent, I_s is the saturation current, V_{pv} is the PV voltage, A is ideality factor, V_T is the thermal voltage, R_s is the series resistance, and R_p is cell shunt resistor.

The second part of the controller is the proposed control strategy, as shown in Figure 3(b). It consists of the PI controller with variable proportional gain, K_p, and integral gain, K_i. The complex relationship between output resistance, irradiance, and PV module temperature with the controller of the PV emulator using the TSIBC with the TSLCF require complicated mathematical equations that are difficult to derive. Therefore, this complex relationship is determine using the artificial neural network. The 146 operating points of the PV emulator is chosen at random where the PI gains are adjusted until the output of the PV emulator is critically damped. These data is trained to determine the function of PI gains with the output resistance and irradiance as the input, as shown in Figure 3(b). The training used the hybrid learning algorithm (the least-squares and back-propagation gradient descent methods) to tune the parameters of a Sugeno-type fuzzy inference system [11]. This relationship is shown in Figure 4(a) and 4(b).

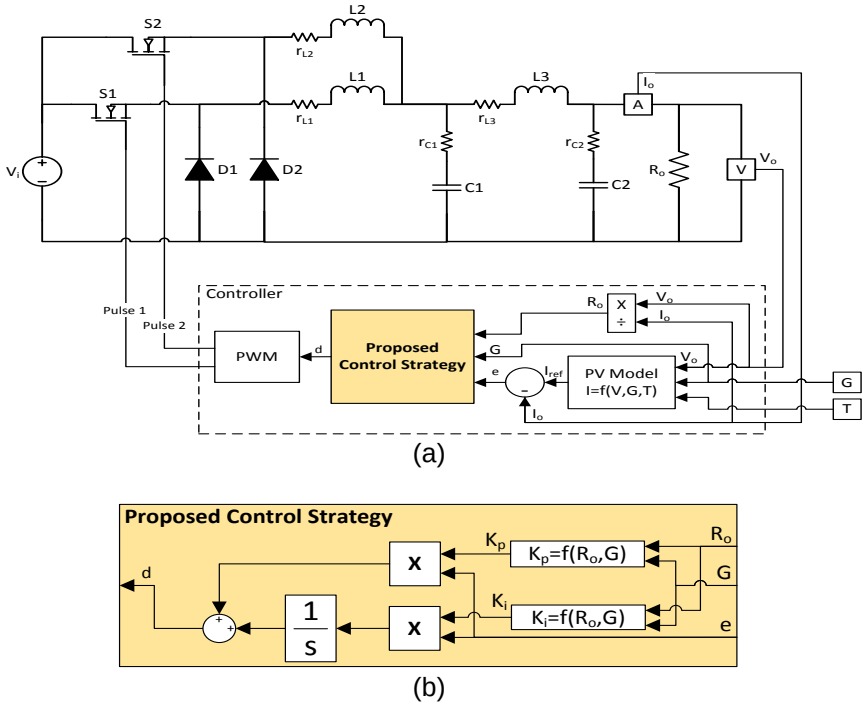

Figure 3. (a) The block diagram of the proposed PV emulator. (b) The block diagram of the adaptive PI controller

The membership function chosen to represent the irradiance dataset is the five Gaussian curve membership functions. Five membership functions are chosen and evenly distributed since the irradiance data collected is at 200 W/m^2, 400 W/m^2, 600 W/m^2, 800 W/m^2, and 1000 W/m^2. The parameter of this membership function is adjusted using the Membership Function Editor in MATLAB. The membership function used to represent the output resistance is more complex compares to the membership function representing the irradiance due to the nonlinear characteristic of the PV module. Three membership functions are used to represent the output resistance. The resistance below 10 Ω is represented using Z-shaped curve membership function. During this condition, the PV emulator operates at constant current region and the PI gains have a similar characteristic. The output resistance between 10 Ω to 20 Ω is represented using Gaussian curve membership function. During this condition, the PV emulator

operates around the boundary of the constant voltage and current regions. The membership function for the output resistance between 20 Ω to 150 Ω is S-shaped curve membership function. During this condition, the PV emulator operates at constant voltage region and the PI gains have a similar characteristic.

The third part in the controller is the pulse width modulator (PWM). The function of the PWM is to generate switching pulses for the MOSFETs depending on the duty cycle. By referring to Figure 3(a), two pulses are sent to the power converter. The pulse 2 is always 180^{o} phase shift from the pulse 1.

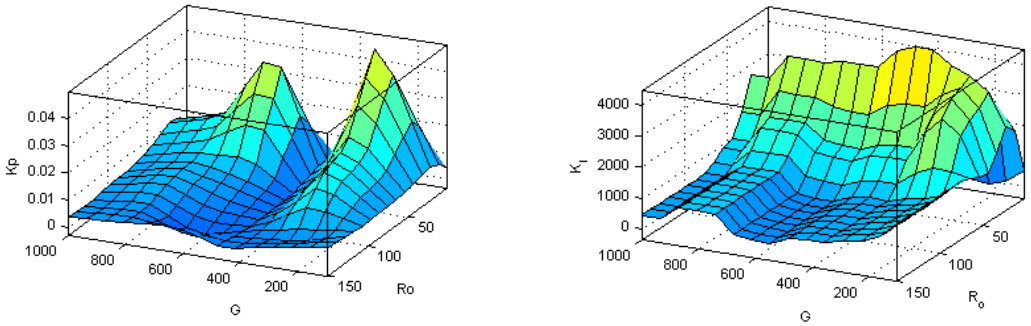

Figure 4. The a) proportional gain, K_p and b) integral gain, K_i surface generated using artificial neural network depending on the output resistor, R_o and irradiance, G

4. Results and Discussions

The accuracy and transient response are the important factors when analyzing the characteristic of the PV emulator. The I-V characteristic curve produced by the PV emulator should be similar with the actual PV module characteristics [4, 12]. The dynamic response of the PV emulator should close to 10th of a microsecond to obtain better results from MPPT devices and power conditioning system [7, 13].

4.1. Accuracy of the PV Emulator

The accuracy of the PV emulator depends on the PV model used. The operating point of the PV emulator has a high accuracy if the PV model is accurate. However, the control strategy also affects the accuracy of the PV emulator where the unstable reference input leads to an inaccurate operating point. The conventional control strategy has a stability problem in the constant voltage region. As a result, the PV emulator output becomes inaccurate when operating in the constant voltage region. However, the proposed control strategy has no stability problem which resulting to a more accurate output.

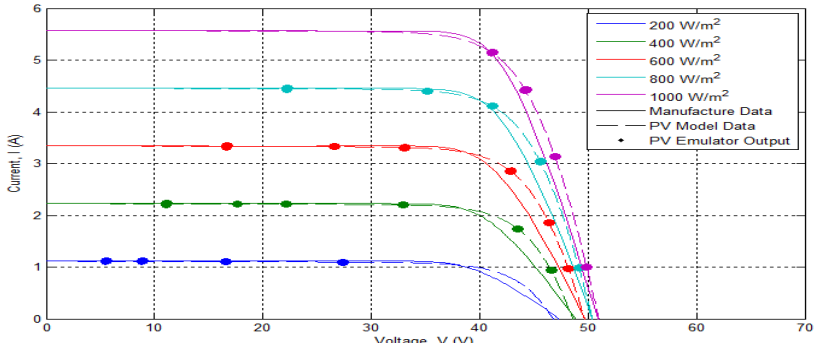

Figure 5. The I-V characteristic curved obtained from the PV model and the manufacturer datasheet compared to the photovoltaic emulator output at 25 ^{o}C

Figure 5 shows the I-V characteristic curve obtained from the manufacturer datasheet, the PV model, and the PV emulator output of the proposed control strategy. The results show the output of the PV emulator is capable of following the I-V characteristic curve of the PV model. However, the inaccurate PV model results in different I-V characteristic curve compared to the manufacturer datasheet.

4.2. Transient Response of the PV Emulator

The adaptive PI controller is designed to maintain a fast and stable transient response even when the output resistance and irradiance are changed. The dynamic performance of the proposed adaptive PI controller is compared with the conventional fixed PI controller method by using the TSIBC with the TSLCF. The conventional fixed PI controller used the constant proportional gain and the integral gain of 2500 and 0.01 respectively.

Figure 6(a) and Figure 6(b) show the data sample of output current from the PV emulator at different load conditions. When the output resistance is between 5 Ω to 50 Ω, the PV emulator operates at the optimum dynamic response. The overall settling time of the PV emulator is maintained around 150 µs even when the output resistance and irradiance are changed. The stability of the PV emulator is also maintained in both constant current region and constant voltage region. This shows that the proposed control strategy is highly adaptive to the load and irradiance change. The output current remains stable and has a fast dynamic response.

The dynamic characteristic of the output current of the conventional method is similar to the proposed control strategy for 5 Ω. This is because the PI controller for the conventional method is designed at 5 Ω. For the output resistance of 10 Ω and 25 Ω, the proposed control strategy produce relatively 60 % to 80 % faster response compared to the conventional method. When the output resistance is 50 Ω, there is approximately 1.8 % output current overshoot for the conventional method. This is due to a large reference input produced by the conventional method during startup. A slow system respond is required to prevent the overshoot. Since the conventional method has the fixed gains, the overshoot could not be eliminated. However, the proposed control strategy able to adjust the gains of the PI controller to prevent the output current overshoot. The adjustment of PI controller gain causing the dynamic performance of the PV emulator to become slow.

In conclusion, the proposed control strategy capable of producing faster transient response compared to the conventional method. For the operation with a large output resistance, the proposed control strategy is also able to eliminate the output current overshoot by adaptively slow down the operation of the PV emulator.

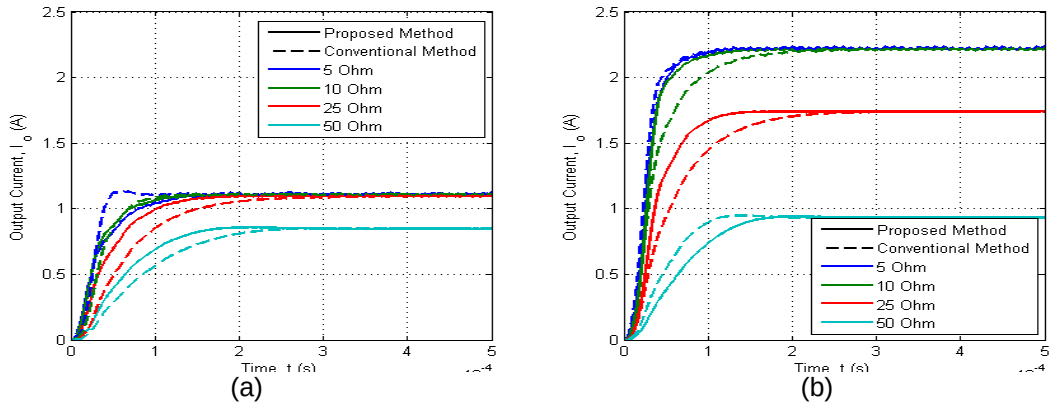

Figure 6. The simulated results of the photovoltaic emulator output current during startup under a) 200 W/m^2 and 400 W/m^2 at 25 ^{o}C with a series of output resistances.

The reference input is stable if the operating point is located in the constant current region, as shown in Figure 7(a) and Figure 7(b). However, if the output resistance increases and the new operating point is located in the constant voltage region, the reference point becomes oscillate.

This effect is shown in Figure 7(a) when the output resistance is increased at 0.6 ms. The reference input is more stable when the output resistance decreases and moving the operating point from the constant voltage region to the constant current region. However, the output voltage of the PV emulator cannot change instantaneously when the load decreases, as shown in Figure 7(d). As a result, the decrease in the output resistance causing the output current spike, as shown in Figure 7(c). A larger output resistance drop causes a larger spike.

Figure 6(a) and Figure 6(b) show the PV emulator system maintains the output current dynamic response even though the output resistance increases. The proposed control strategy shows that the integral gain becomes lower after 20 Ω to maintain a stable reference input, as shown in Figure 4(b). The factor causing a fast dynamic response when the PV emulator operates in the constant voltage region is the PV model. When the PV emulator is started, the output voltage is zero. As a result, the reference input is equal to the short circuit current of the PV at given irradiance and module temperature. The reference input produced is larger than the operating point corresponding to the output resistance, as shown in Figure 7(c). The error, e, produces is large causing the PV emulator system to produce a fast dynamic response. As the voltage increases, the reference current becomes lower, as shown in Figure 7(c). The error becomes smaller and the PV emulator reaches the steady state condition without any instability and producing a fast dynamic response.

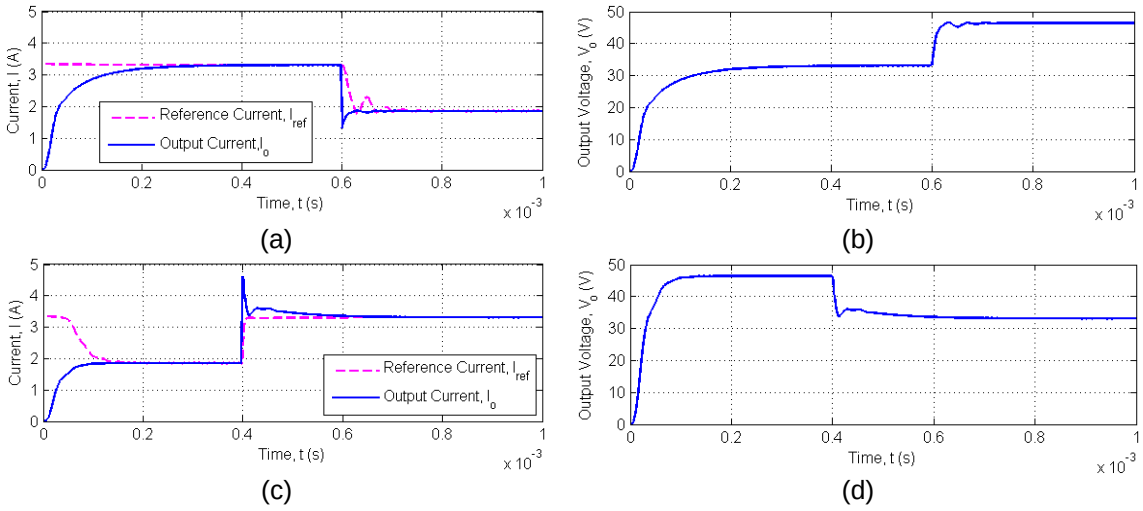

Figure 7. The simulated results of the PV emulator under 600 W/m^2 and 25 ^{o}C. The output resistance, R_o was step-changed from 10 Ω to 25 Ω at 0.6 ms where (a) the reference current, I_{ref} and the output current, I_o with (b) the output voltage, V_o of the PV emulator. The R_o was step-changed from 25 Ω to 10 Ω at 0.4 ms where (c) the I_{ref} and the I_o with (d) the V_o of the PV emulator

5. Conclusion

The conventional control strategy uses the closed-loop power converter system to determine the operating point of the PV emulator. According to the Final Value Theorem, the steady state error of this system is zero. Therefore, the PV emulator output is highly accurate if a good PV model is used. However, the closed-loop power converter system becomes unstable when it is converted into the PV emulator using the conventional control method. As a result, the output of the PV emulator oscillates and the accuracy is reduced. The proposed control strategy overcomes the stability problem faced by the conventional control strategy. Therefore, the PV emulator using the proposed control method is highly accurate.

The simulations show the dynamic response of the converter becomes slow when output resistance becomes high. The PI gains increase as the output resistance increases. However, if the operating point is located in the constant voltage region of the PV I-V characteristic curve, the PI gains is decreased to prevent instability of the system. The artificial neural network control strategy is able to determine the complex relationship between the output

resistance and the irradiance with the PI gains. The adaptive PI controller maintains the dynamic performance of the PV emulator even when the output resistance and the irradiance are varied. The output current overshoot of the PV emulator when a large output resistance is connected to the PV emulator is eliminated when using the proposed control strategy. This condition is caused by a large reference input produces by the PV model. The movement of operation from the constant current region to the constant voltage region causing the PI controller to respond faster. The adaptive PI controller automatically reduced the integral gain to prevent the overshoot. Even though the proposed control strategy able to produce a fast and stable output, the flexibility of this method is low.

The constant current and voltage regions are different corresponding to the output resistance and irradiance due to the different I-V characteristic of the different PV modules. Therefore, the critically damped and overdamped operation change. As a result, the training of the PI gains is conducted again to allow the PV emulator to operate properly. The training of the different PV modules requires the different parameters of the output resistance membership function. Therefore, the parameters tuning of the membership function need is necessary which increase the complexity of the proposed control strategy.

Acknowledgements

The authors would like to pay gratitude to Universiti Teknologi Malaysia (UTM) for supporting with lab and library facilities. In addition, the authors would like to express their appreciation to the Ministry of Higher Education, Malaysia (MOHE). They also acknowledge funding provided by fundamental research grant scheme (FRGS) under vote 4F596, Universiti Teknologi Malaysia (UTM).Lastly thanks to those colleagues who have either directly or indirectly contributed to the completion of this work.

References

[1] MC Di Piazza, M Pucci, A Ragusa, G Vitale. Analytical Versus Neural Real-Time Simulation of a Photovoltaic Generator Based on a DC-DC Converter. *IEEE Transactions on Industry Applications.* 2010; 46: 2501-2510.
[2] González-Medina, Raúl Patrao, Iván Garcerá, Gabriel Figueres, Emilio. A low-cost photovoltaic emulator for static and dynamic evaluation of photovoltaic power converters and facilities. *Progress in Photovoltaics: Research and Applications.* 2014; 22: 227-241.
[3] A Vijayakumari, AT Devarajan, N Devarajan. Design and development of a model-based hardware simulator for photovoltaic array. *International Journal of Electrical Power & Energy Systems.* 2012; 43: 40-46.
[4] A Koran, T LaBella, JS Lai. High Efficiency Photovoltaic Source Simulator with Fast Response Time for Solar Power Conditioning Systems Evaluation. *IEEE Transactions on Power Electronics.* 2014; 29: 1285-1297.
[5] A Koran, K Sano, K Rae-Young, L Jih-Sheng, Design of a Photovoltaic Simulator With a Novel Reference Signal Generator and Two-Stage LC Output Filter. *IEEE Transactions on Power Electronics.* 2010; 25: 1331-1338.
[6] Y Kim, W Lee, M Pedram, N Chang. Dual-mode power regulator for photovoltaic module emulation. *Applied energy.* 2013; 101: 730-739.
[7] K Nguyen-Duy, A Knott, MAE Andersen. High Dynamic Performance Nonlinear Source Emulator. *IEEE Transactions on Power Electronics.* 2016; 31: 2562-2574.
[8] J Zhang, S Wang, Z Wang, L Tian. Design and realization of a digital PV simulator with a push-pull forward circuit. *Journal of Power Electronics.* 2014; 14: 444-457.
[9] MG Villalva, JR Gazoli. Comprehensive approach to modeling and simulation of photovoltaic arrays. *Power Electronics, IEEE Transactions on.* 2009; 24: 1198-1208.
[10] Sanyo. Sanyo HIT photovoltaic module. Stahlgruberring, Munich, Germany: SANYO Component Europe GmbH, Solar Division. 2009.
[11] ANFIS: Training routine for Sugeno-type fuzzy inference system. 2014.
[12] KH Tang, KH Chao, YW Chao, JP Chen. Design and implementation of a simulator for photovoltaic modules. *International Journal of Photoenergy.* 2012; 2012.
[13] R Kadri, H Andrei, JP Gaubert, T Ivanovici, G Champenois, P Andrei. Modeling of the photovoltaic cell circuit parameters for optimum connection model and real-time emulator with partial shadow conditions. *Energy.* 2012; 42: 57-67.